

Change of direction of overthrust shear in the Helvetic nappes of western Switzerland

DOROTHEE DIETRICH

Geologisches Institut, ETH-Zentrum, CH-8092 Zürich, Switzerland

and

DAVID W. DURNEY

School of Earth Sciences, Macquarie University, N.S.W. 2113, Australia

(Received 1 July 1984; accepted in revised form 7 February 1985)

Abstract—The lowest of the Helvetic nappes in western Switzerland, the Morcles and the Doldenhorn nappes, are large-scale recumbent folds in equivalent tectonic positions in the Alpine chain. A comparison of the orientations of stretching lineations in both nappes shows that the lineations in the two stratigraphically normal sequences trend N–S, whereas those in the two stratigraphically inverted sequences trend NW–SE.

A similar geometrical relationship has been found from an analysis of the calcite *c*-axis directions of these limestones: the two normal sequences show NW–SE directed *c*-axes, whereas the two inverted sequences show W–E directed *c*-axes. These observations lead to the following conclusions: (1) Regionally consistent shear movements occurred over a strike distance of more than 60 km, and these gave rise to similar deformation patterns in both nappes. (2) A progressive rotation of these shear movements from a northerly direction in the earlier-formed limbs to northwesterly in the later-formed inverted limbs can be deduced. The finite-strain stretching lineations lag behind the crystallographic fabric axes formed in the later part of the deformation history.

INTRODUCTION

How CAN small-scale deformational structures be related to the overall directions of nappe transport? What are the overthrust directions in the Helvetic nappes? How regionally constant are these directions? We will try to answer these questions using observations on stretching lineations, microstructures in limestones, and crystallographic preferred orientations of calcite.

The Morcles and the Doldenhorn nappes are huge recumbent fold nappes which have comparable geometrical positions in the pile of the Helvetic nappes of the western Swiss Alps (Fig. 1). The Morcles nappe overlies the autochthonous sequence of the Aiguilles Rouges massif, and the Doldenhorn nappe overlies the autochthonous cover of the Eastern massif. Figures 2 and 3 show the overall geometrical aspects of the two nappes, illustrating their similarity. In fact they were first correlated across the Wildstrubel depression by the early workers in the region (e.g. Arbenz in Heim 1921, p. 443).

A key problem in any kinematic analysis of a mountain chain is the choice of overthrust model. Did the nappes evolve from top to bottom or vice versa, that is were the geometrically highest nappes the first to be formed, or the last? In the Helvetic nappes of western Switzerland we do not observe structures of geometrically lower nappes being cut by the overthrusting of higher nappes, and we deduce a top-to-bottom formation model. Incremental strains determined from pressure-shadows also point towards an evolution of strain from that seen in the

older higher nappes towards that seen in the lower younger ones (Durney & Ramsay 1973, Fig. 22, and unpublished data by D. Dietrich). This development sequence and overall strain pattern agrees with the simple-shear models proposed for the evolution of the Doldenhorn nappe by Laubscher (1983) and for the evolution of the Helvetic fold-thrust belt by Ramsay *et al.* (1983). However, it is clear that, in detail, the simple-shear model is insufficient to account for all the complex geometric features seen in the nappes (Casey *et al.* 1983, Dietrich (in review), Gray & Durney 1979, Ramsay 1981, Ramsay & Huber 1983 pp. 276–278, Siddans 1983).

CONSTRAINTS FOR A KINEMATIC MODEL ARISING FROM THE LINEATION PATTERN

Both the Morcles and Doldenhorn nappes have a well developed slaty cleavage which decreases in intensity from the internal part of the nappes, or root zone, towards the external part of the nappes. This cleavage is arranged in an axial-planar or fan-like manner in relation to the principal folds of the nappes and is therefore genetically linked to the overall nappe structure. Where the slaty cleavage is well developed a stretching lineation can be observed on the cleavage planes of the competent limestone layers. This lineation is generally parallel to the *X*-axis of the finite-strain ellipsoid as determined from pressure-shadows, deformed pebbles, ooids, fossils, and elongated streaks (Durney 1972). At several

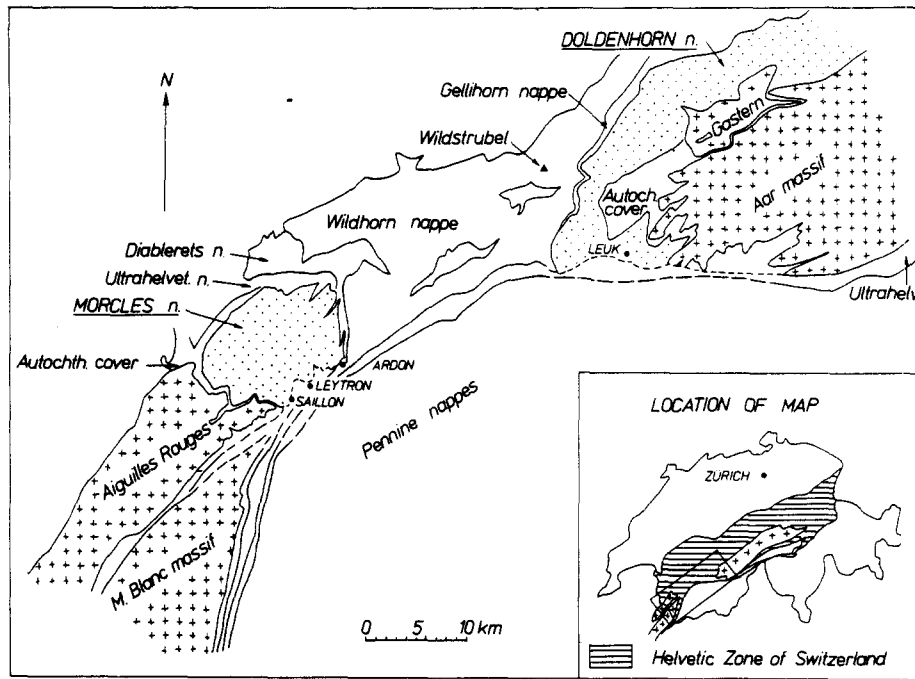


Fig. 1. Tectonic sketch map of the Helvetic nappes of western Switzerland.

localities in the root zone of the Helvetic nappes two distinct stretching lineations coexist, one being more strongly developed than the other. Where two lineations coexist, the more strongly developed lineation may not coincide exactly with the *X*-axis. An example is described by Durney (1972, fig. 30) from the Liassic core of the Morcles nappe at Leytron. Figures 4 and 5 are stretching lineation maps of the Morcles and Doldenhorn nappes.

In the Morcles nappe (Fig. 4) the stretching lineations have a general N-S direction in the stratigraphically normal sequence which outcrops at and to the north of Ardon, and a regular NW-SE direction in the inverted sequence cropping out at and to the northwest of Saillon. There appears to be a gradual transition between the two directions in the core of the nappe, N of Saillon. No overprinting relations are known between the N-S and the NW-SE lineations. At some localities a third direction, NE-SW, exists (e.g. Leytron). Where this occurs,

the NE-SW trending lineation overprints the N-S and the NW-SE trending lineations. A late timing for the NE-SW stretching is also demonstrated by the growth sequence of extension fibres in pressure-shadows and chocolate-tablet boudins (Durney & Ramsay 1973, Casey *et al.* 1983).

In the Doldenhorn nappe (Fig. 5) there are comparable differences between the lineation directions in the normal and the inverted sequences. A general N-S trending lineation can be observed in the normal limb of the nappe around Leuk. The inverted sequence, exposed below the top of the Hockenhorn, shows NW-SE trending lineations. In this nappe a gradual transition between the two directions can also be seen (e.g. in the northern, frontal part), but no overprinting relations are known between the N-S and the NW-SE lineations. In the southern part of the nappe a third lineation trends NE-SW and overprints the more strongly developed N-S trending lineation. This structure has been inter-

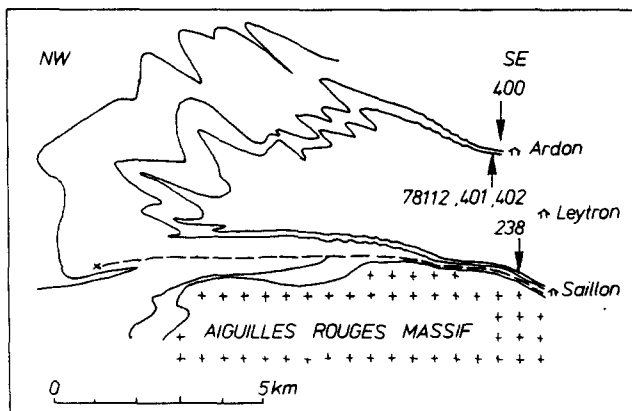


Fig. 2. A profile (down-plunge projection) through the Morcles nappe. The positions of the specimens analysed are indicated.

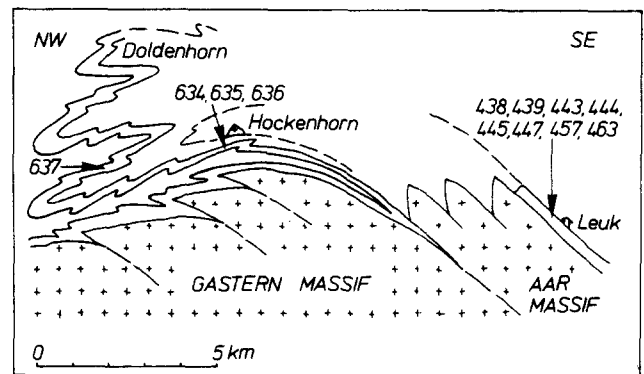


Fig. 3. A synthetic cross-section of the Doldenhorn nappe, modified after Schläpfi in Trümpy (1980). The positions of the specimens analysed are indicated.

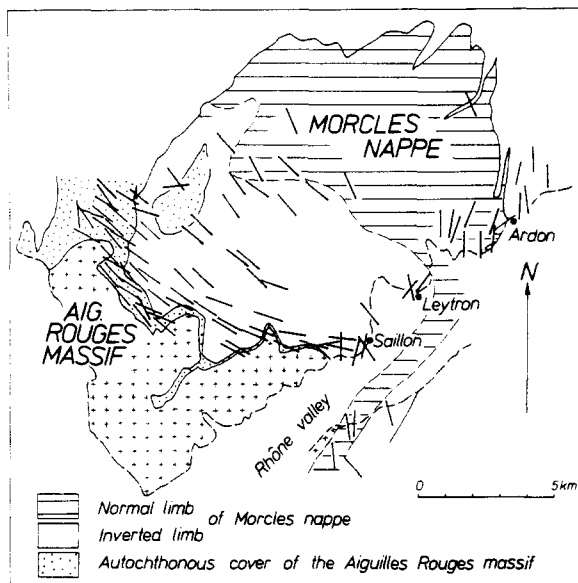


Fig. 4. A stretching lineation map of the Morcles nappe. Information on the dips of the cleavage plane and the plunges of the lineations is contained in Fig. 11.

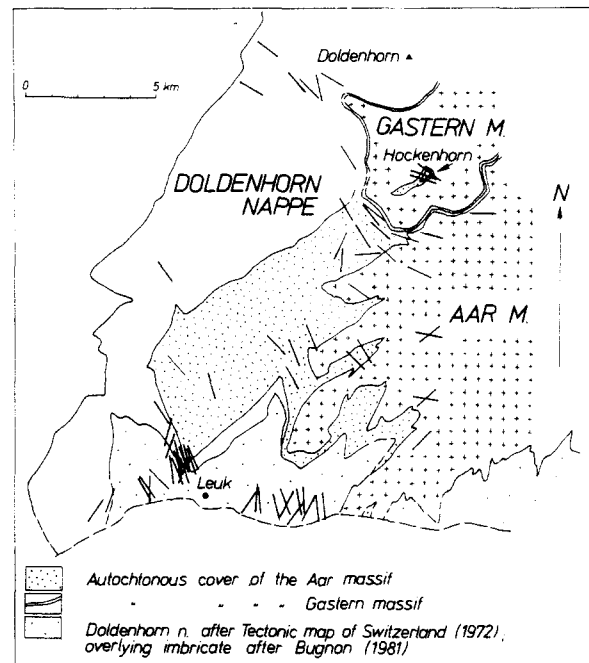


Fig. 5. A stretching lineation map of the Doldenhorn nappe. Some of the stretching lineations between the Torrenthorn and the Löttschenpass (middle part of the figure) are from Schläppi (1980). The stretching lineations in the Aar massif are from Steck (1984).

interpreted as an intersection lineation between the pervasive cleavage and a later second-phase cleavage (Masson *et al.* in Trümpy 1980). But since the relative timing of these two lineations corresponds with the growth sequence of extension fibres in pressure-shadows, we consider both lineations to be stretching lineations. The two nappes therefore show similar lineation patterns. Steck (1984) has presented stretching lineation data for the Aar massif and these show comparable directions to the data presented here. His older lineations trend NW–SE and correspond to those on the inverted limb. His younger lineation trends NE–SW.

For simple-shear deformation with constantly oriented shear planes and shear direction, the extension direction of finite strain tends to become parallel to the shear direction at large shear strains (Ramsay 1967, Fig. 3.22). Thus the stretching lineation direction gives the direction of the overthrust shear movements. If we accept the shear model proposed for the development of the Doldenhorn nappe (Laubscher 1983), as well as the results from numerical modelling, which show that the overall fold geometry of the Morcles nappe can be related to heterogeneous simple shear (Casey & Huggenberger 1985), we can, on the basis of the lineation data, define a change in the overthrust shear direction from the earlier formed normal limbs to the later formed inverted limbs of the two nappes. The shearing associated with the overthrusting and the formation of the two normal limbs had an essentially northwards displacement direction. In its subsequent development the overthrusting rotated in an anticlockwise sense towards W, and the shearing was confined to the overturned limb. Since we have similar lineation directions in both nappes, we conclude that these shear movements were regionally parallel over a distance along strike of at least 60 km, but probably more.

CONSTRAINTS ARISING FROM THE MICROSTRUCTURES AND TEXTURES

How can observations regarding microstructures and textures be integrated in such a kinematic model? An interpretation of the Helvetic root zone, based on correlation of stretching lineations and calcite preferred orientations has been attempted by Dietrich *et al.* (1981). Schmid *et al.* (1981), Schmid (1982) and Dietrich & Song (1984) discuss extensively the nature and tectonic significance of microstructures and textures of the limestones of the western Helvetic nappes. We can summarize these three articles as follows.

(1) Annealing recrystallization is virtually absent from the specimens studied in this part of the Helvetic zone. The microfabric therefore relates directly to the deformation history.

(2) The axes of the microfabric (long, intermediate and short axes of the grains) are not parallel to the axes of the finite-strain ellipsoid as defined by the cleavage plane (finite X and Y directions in the cleavage plane, X parallel to the stretching lineation, finite Z direction perpendicular to the cleavage plane). The obliquity of the grain-shape fabric systematically departs from the orientation of the cleavage in a way that relates to the sense of the overthrust movements.

(3) The axial ratios of the grains vary in the region studied from $x:z = 1.2:1$ to $x:z = 5:1$. In contrast to these values, the finite-strain $X:Z$ ratios from the corresponding localities are orders of magnitude higher. For example at Ardon in the Morcles nappe (Fig. 4) the grain-shape ratio is 5:1, whereas the finite-strain ratio is 440:1 ($1 + e_1 = 21$, calculated from pressure-shadows,

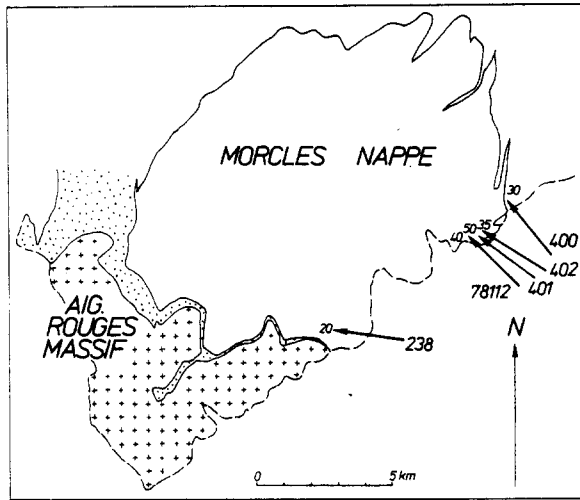


Fig. 6. Calcite *c*-axis directions in the Morcles nappe. Specimen 78112 was measured by S. Schmid.

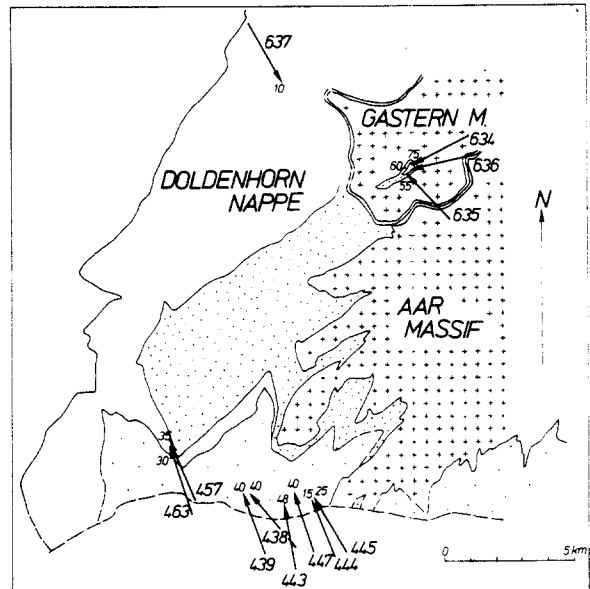


Fig. 7. Calcite *c*-axis directions in the Doldenhorn nappe.

and assuming that $1 + e_3 = 1/(1 + e_1)$ and $1 + e_2 = 1$).

(4) Texture goniometry has been applied to determine the regional orientation of the calcite *c*-axes in the Morcles and Doldenhorn nappes. Instead of measuring the *c*-axis orientation directly, the poles to calcite *a* or (11 $\bar{2}$ 0) planes were measured. This is because the intensity of the *a* diffraction peak is much higher than the intensity of the *c* or (0001) diffraction peak, and therefore easier to measure. The *c*-axis maximum coincides with the *a*-minimum in the pole figures obtained. The correctness of this deduction has been shown by direct measurements of the *c* crystallographic axes by U-stage and by texture goniometry methods (Dietrich & Song 1984, Schmid *et al.* 1981). In the two nappes essentially only one type of texture pattern has been found: the poles to the *a*-planes define great circles which are subparallel to the *xy* plane or flattening plane of the individual grains. Hence the *a*-minima or *c*-maxima obtained are subperpendicular to the flattening planes of the grains.

One important result of these studies is therefore that the finite-strain fabric and the microstructural and textural fabrics are not parallel. Two interpretations of this non-coincidence have been suggested.

(a) Grain shape and texture only record the last strain increment of a continuous shear deformation. These features would be due to grain-boundary migration and/or syntectonic recrystallization (Schmid *et al.* 1981).

(b) Grain-shape and crystallographic fabric relate only to the strains arising during a deformation event that was later than the formation of the macroscopically predominant cleavage. The grain-shape fabric would therefore correspond to a second-phase cleavage (Dietrich & Song 1984).

A study of calcite preferred orientation around first- and second-phase folds of the Morcles nappe has shown that the preferred orientation is related to the cleavage fan of second-phase folds. In a second-phase fold at Saillon, which deforms the macroscopically predominant cleavage, the following geometrical relationships are observed: the flattening plane defined by the grain-

shape fabric is everywhere parallel to the cleavage fan of the second-phase fold. The inferred *c*-axis maxima are perpendicular to the grain-shape fabric (Dietrich, in review). Thus, generalizing, we assume interpretation (b) as a working hypothesis.

Figures 6 and 7 show the azimuths of the *c*-axis maxima obtained for the two nappes. The *c*-axis directions are inferred from calcite *a* pole figures, which were measured by X-ray texture goniometry. (For the measurement method see Casey *et al.* 1978 and Schmid *et al.* 1981. A more detailed discussion of the pole figures obtained can be found in Dietrich & Song 1984.)

In the normal limb of the Morcles nappe, specimens 401, 402, 78112 (Fig. 6) show an overall NW direction of the *c*-axis maxima. The *c*-axis maximum in the overlying Diablerets nappe (specimen 400) has the same orientation. At one locality situated in the inverted limb of the Morcles nappe the *c*-maximum (specimen 238) shows a westwards direction.

The *c*-axis directions in the normal limb of the Doldenhorn nappe, specimens 438, 439, 443, 444, 445, 447, 457, 463, 637 (Fig. 7), also trend NW. Two of the three analyses of limestones from the inverted limb of the Doldenhorn nappe, specimens 634 and 636, show a westwards trend. The pattern of these inverted-limb pole figures is discussed more fully below.

The fabric axes from the normal limbs of the Morcles and Doldenhorn nappes are mutually parallel, and the same is true of those from the inverted limbs. We therefore conclude that the shear movements that gave rise to similar texture patterns in the equivalent limbs of the two nappes had identical directions.

FABRICS FROM THE INVERTED LIMB OF THE DOLDENHORN NAPPE

The inverted sequence of the Doldenhorn nappe plus the autochthonous cover of the Gastern massif appear to

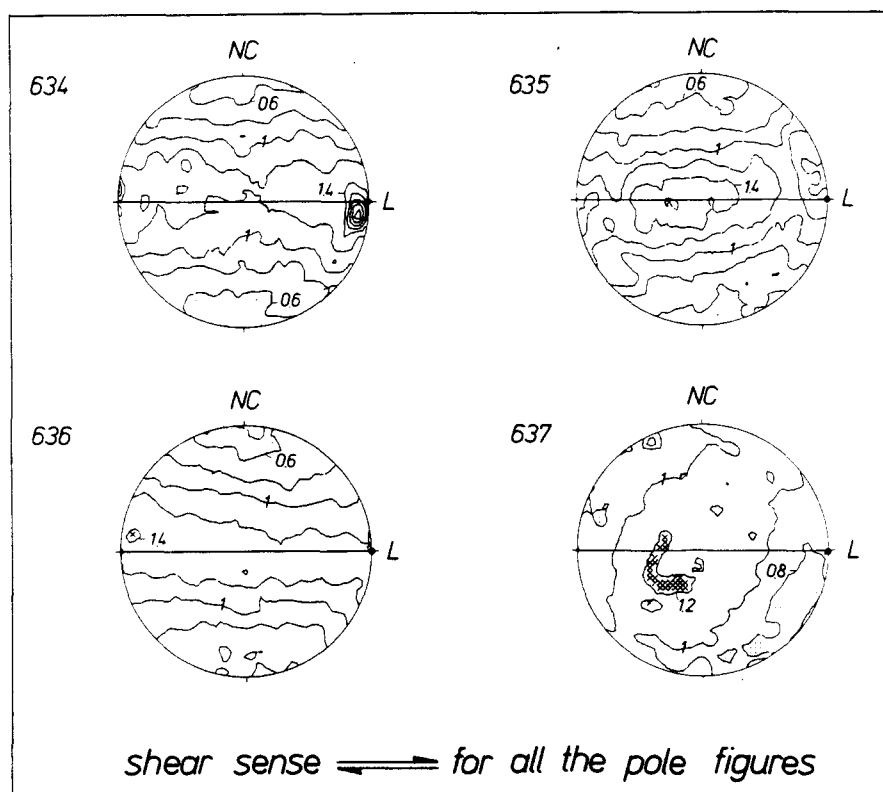


Fig. 8. Pole figures of calcite a -planes, measured parallel to the stretching lineation and perpendicular to the cleavage. Upper hemisphere equal-area projection. L, stretching lineation; NC, normal to the cleavage. 634, 635 and 636 are from the inverted limb of the Doldenhorn nappe. 637 is from the external part of the normal limb. The shear sense relative to all the pole figures is dextral. The stipple pattern indicates the region of the a -minimum or of the c -maximum. The contour interval is 0.2; the contours represent multiples of an uniform distribution. The intensity maxima are 2.3 for 634, 1.6 for 635, 1.4 for 636, 1.3 for 637.

be pinched in between the Gastern and Aar crystalline massifs (Fig. 3). The sedimentary cover of the Gastern massif has a maximum thickness of 20 m. The inverted Doldenhorn limb comprises Triassic to Upper Jurassic sediments, and is also about 20 m thick in the Hockenhorn region. For comparison, in the normal limb sequence at the Doldenhorn (mountain peak indicated in Figs. 3 and 5), the same stratigraphic interval measures at least 500 m.

The Upper Jurassic of the inverted-limb sequence consists of about 7 m of strongly deformed limestones. These limestones have been found suitable for a texture goniometer study. Since the results obtained show some aspects which differ from the typical pattern of calcite preferred orientation in the western Helvetic nappes, they are discussed here.

The limestones investigated are located west of the Kleinhockenhorn (specimen 635) and beneath the top of the Hockenhorn (specimens 634 and 636). They belong to a thin sedimentary layer between the crystalline top of the Hockenhorn, which can be correlated with the Aar massif, and the underlying Gastern granite (Fig. 3). These limestones are intensely deformed and show well developed wavy cleavage surfaces, with a cm-spacing. Pressure-shadows from the geometrically overlying Triassic have given finite-strain values of $1 + e_1 = 10$, but these are indicative only of the solution-transfer part of the deformation history.

Figure 8 shows the pole figures measured from these sediments (634–636) and, for comparison, a pole figure measured from a normal limb in the frontal zone of the Doldenhorn nappe (637, see also Fig. 3). The shear sense, inferred from the direction of tectonic transport, is dextral with respect to all four pole figures. In all pole figures a clear a -minimum or c -maximum is visible. The position of the c -maximum in 637 differs from those of the inverted-limb pole figures. 634, 635 and 636 show calcite a -girdles with a very low degree of obliquity in relation to the cleavage (indicated with a horizontal line). Therefore no clear sense of shear can be inferred from the pole figures. This is in contrast with the generally clear obliquity between the a -girdles and the cleavage found in the western Helvetic nappes (Dietrich & Song 1984). Similar symmetric pole figures have been obtained for the Lochseiten mylonite beneath the Glarus overthrust (Schmid *et al.* 1981). Specimen 637 shows a clearly oblique texture in accordance with the shear sense. The preferred orientation in this specimen is weaker than in the other three, in relation to the more external position in the nappe of 637.

Figure 9 shows micrographs illustrating the microstructures of specimens 635 and 637. The micrographs are taken from thin sections parallel to the stretching lineation and perpendicular to the cleavage; the macroscopically predominant cleavage is horizontal in all cases. In Fig. 9(a) there is an evident obliquity between

the matrix grains and the cleavage. The matrix grains show a higher degree of obliquity than the bigger intraclasts present. The flattening plane as defined by the matrix grains is deflected around the intraclasts. The fact that the great circles in the corresponding pole figures of specimens 634–636 do not correspond with the observed obliquity of the matrix grains, can be explained in accordance with Schmid (1982) as the result of the greater statistical (volumetric) influence of the coarser grains on the pattern obtained from texture goniometry. The matrix grains are mostly untwinned, whereas the bigger intraclasts are heavily twinned. Figure 9(b) shows a twinned intraclast with deformed twin lamellae.

Subgrain formation is very common in the bigger grains. Nucleation of new grains of an extremely small grain size can be observed particularly clearly in the intraclasts (Fig. 9c). This reflects an early stage of the process of recrystallization by nucleation, as would be found in the initial stages of progressive mylonitization.

Figures 9(d) and (e) show, for comparison, the microstructure of the external normal limb limestones. The mean grain size is much smaller than in 635, possibly indicating a lower degree of metamorphism. Twinning is absent (Fig. 9e). A comparison of the grain-shape fabric with the corresponding pole figure shows that the great

circle of *a*-axes and the long axes of the matrix grains have the same sense of obliquity with respect to the macroscopic cleavage. However, an exact comparison of the two fabrics is difficult because of the relatively poorly defined great circle of *a*-axes.

In Fig. 10 the pole figures of Fig. 8 are represented in geographical coordinates. The inferred *c*-maxima in 634–636 have a comparable position. The variation in the inverted-limb *c*-axis azimuths of Fig. 7 becomes emphasized only as a result of the steep plunge of the vectors. Again, the position of the *c*-maxima in specimens 634–636 differs from 637.

For 635 and 636 the grain flattening plane has been constructed using the angle of obliquity of the matrix grains with respect to the macroscopic cleavage in two perpendicular thin sections, labelled A and B in Fig. 10. Section A is parallel to the stretching lineation and perpendicular to the cleavage, whereas section B is perpendicular to stretching lineation and cleavage. The flattening planes of the matrix grains do not coincide with the *a*-girdles. This is also in contrast with all the other pole figures of *a*-axes from the Helvetic nappes of western Switzerland, where the great circles of *a*-axes are subparallel to the grain flattening planes (Dietrich & Song 1984). The great circles are instead subparallel to

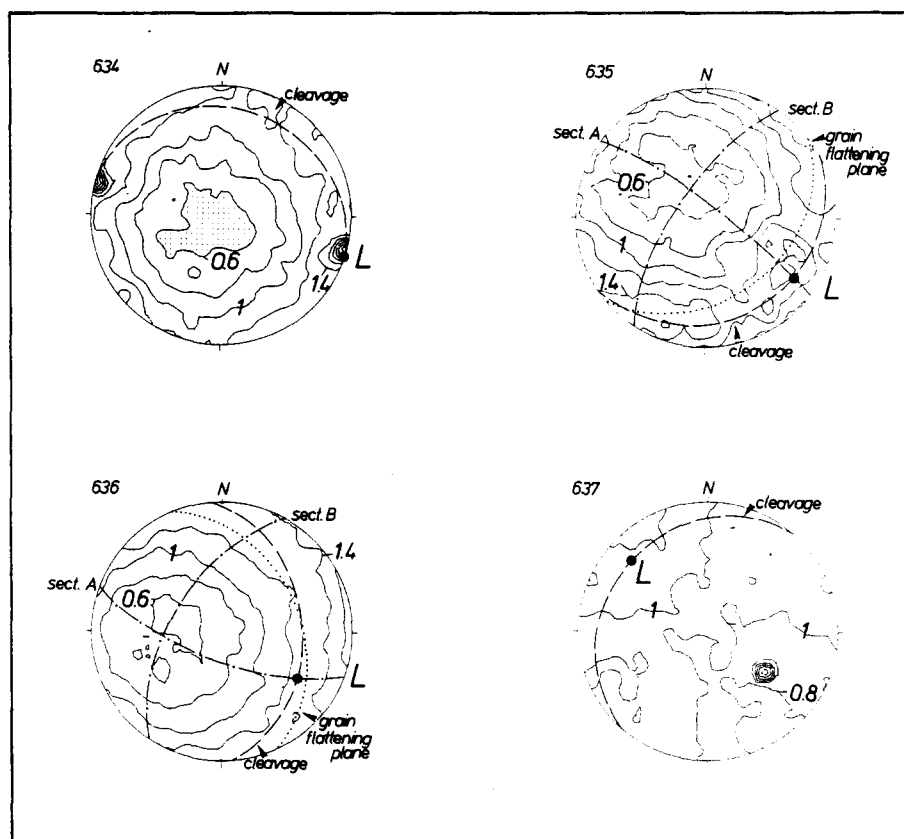


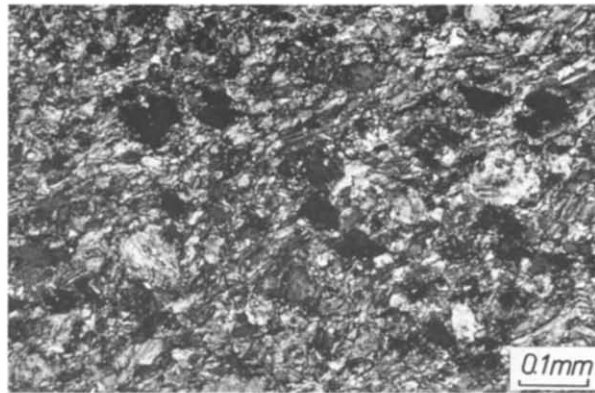
Fig. 10. Pole figures of calcite *a*-planes from specimens of the inverted limb of the Doldenhorn nappe (634, 635, 636) and from the external part of the normal limb (637). The pole figures are in lower hemisphere equal-area projection, and rotated so that the north point of the pole figure coincides with geographical north. The rotation of the pole figures has been performed using a computer program by M. Casey. L, stretching lineation. The stipple pattern indicates the region of the *a*-minimum or of the *c*-maximum. The contour interval is 0.2; the contours represent multiples of a uniform distribution. The intensity maxima are 2.6 for 634, 1.6 for 635, 1.4 for 636, 1.9 for 637. The difference in value of the intensity maxima in the rotated and unrotated pole figures of 634 and 637 is an artefact of the contour smoothing process. The *a*-maximum visible in the SE quadrant of 637 (and on the periphery of 637 in Fig. 8) is due only to the statistical effect of an individual bigger intraclast present in the specimen.

shear sense

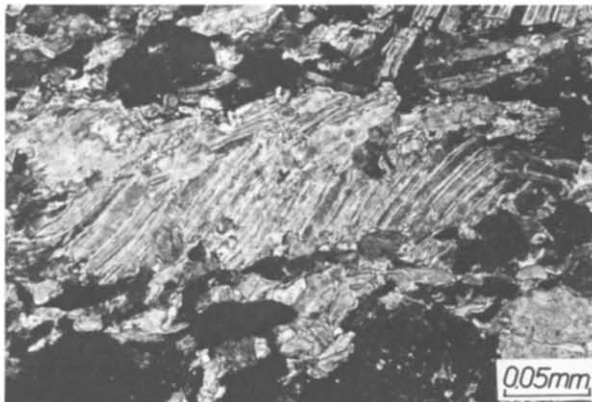


for all the micrographs

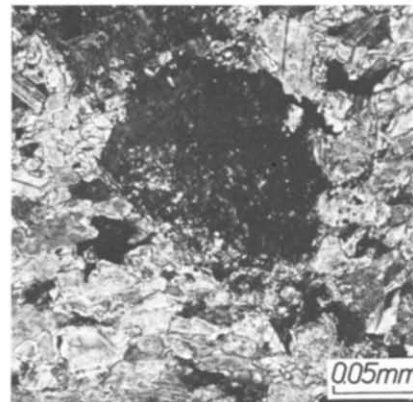
a. 635



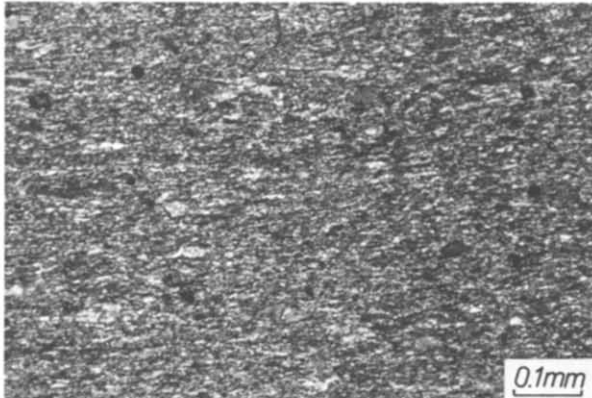
b. 635



c. 635



d. 637



e. 637

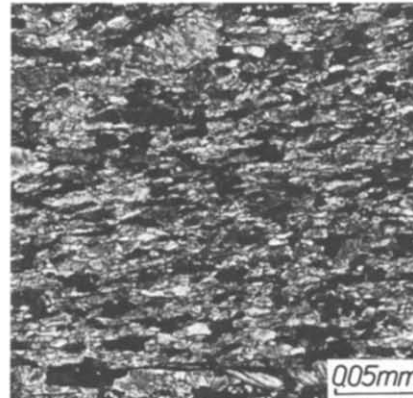


Fig. 9. Photomicrographs of specimens 635 and 637 from Upper Jurassic limestones of the Doldenhorn nappe. The orientation of all the micrographs is parallel to the stretching lineation and perpendicular to the macroscopic cleavage. The cleavage is therefore horizontal in all the micrographs. (a) The grain shape fabric seen in 635 shows an obliquity clearly defined by the matrix grains relative to the cleavage. The intraclasts do not show such an obliquity. (b) Enlargement of (a) showing a twinned intraclast with deformed twin lamellae. (c) An intraclast with newly nucleated small grains. (d) Microstructure from 637 indicating a lower degree of metamorphism: a mosaic of small, slightly flattened grains which do not show a strong obliquity relative to the cleavage. (e) Enlargement of (d) showing the lack of twinning.

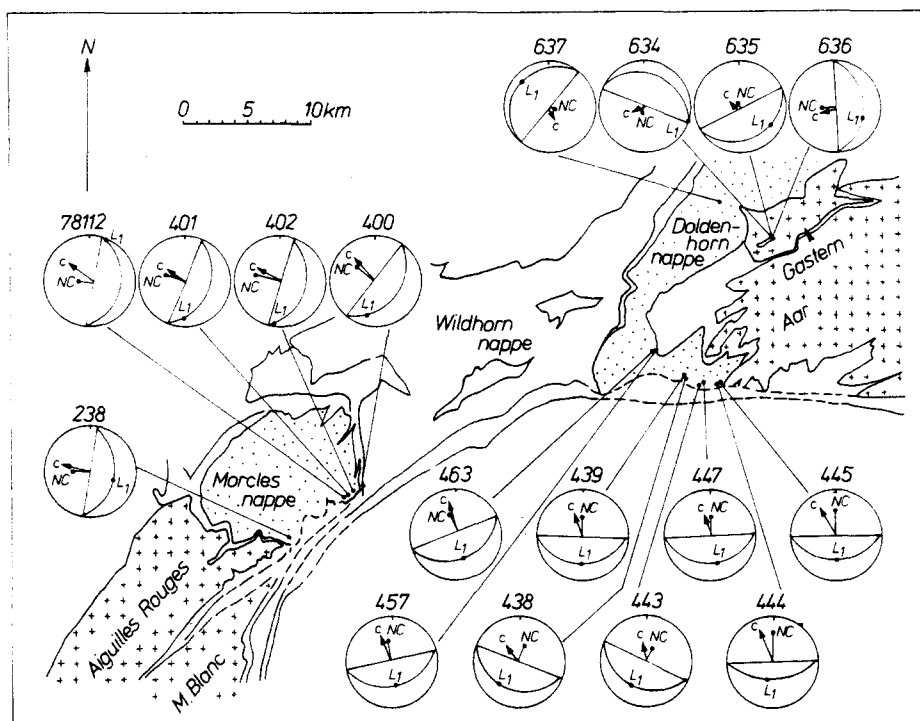


Fig. 11. Synoptic equal-area projections (lower hemisphere) indicating the principal fabric elements for the region studied. The cleavage planes, or finite-strain XY planes, are indicated together with the main stretching lineations, or finite strain X -directions (L_1). The arrows indicate the c -axis maxima (c) obtained by texture goniometry. They are clearly oblique to the normal to the cleavage (NC), except in the inverted limb of the Doldenhorn nappe (see discussion in text). The crystallographic fabric can therefore be related to a second phase of deformation, which contributes to the finite strain, but which is clearly oblique to it. The shear sense associated with the obliquity of the crystallographic fabric is from the c -axis maximum towards the normal to the cleavage. In the normal limb projections this direction is subparallel to the direction of L_1 in the inverted limbs of the two nappes. After Dietrich *et al.* (1981).

the macroscopic cleavage, that is, to the XY plane of finite strain (Fig. 8). It is interesting that in both specimens the constructed grain flattening plane is rotated anticlockwise towards the west in relation to the a -girdles. The obliquity of the matrix grain-shape fabric results from the last deformation event, and represents the second-phase cleavage in these rocks. The fabric bears, therefore, indications of the progressive evolution of the deformation: these pole figures record an anticlockwise rotation of the overthrust shear.

CONCLUSIONS

The stretching-lineation patterns represent the finite-strain fabric in the Morcles and in the Doldenhorn nappes. These lineations trend N-S in both normal sequences, and NW-SE in both inverted sequences of these nappes. Because of the intensity of the geometrically related strain it is deduced that they are closely aligned with the shear direction produced by nappe transport. The microfibrils (microstructures and calcite preferred orientations) record a second deformation event which overprints the principal fabric that was formed in the first phase of deformation. This second deformation must also contribute to the finite strain. The c -axis directions can be used to define the late compression directions which appear to correspond to the late transport directions. The c -axis directions are

NW in the two normal sequences, and W in the two inverted sequences. Thus the crystallographic fabric axes appear to be systematically rotated in an anticlockwise sense relative to the corresponding finite-strain lineation direction. This is very clear from the synoptic stereograms in Fig. 11. In fact the crystallographic fabric directions in the two normal sequences are parallel to the stretching-lineation directions in the two inverted sequences. Regionally, shear movements for the two normal sequences can be deduced to be parallel, and those for the two inverted sequences can also be deduced to be parallel (Fig. 12). These shear movements rotated from a northward towards a westward direction. Evidence for such an anticlockwise rotation can also be deduced from incremental strain data determined by an analysis of extension fibres in pressure-shadows (Durney & Ramsay 1973). As the movement direction rotated, the locus of the principal deformation migrated down through the nappes, being localized first in the two normal limbs, then in the two inverted sequences.

The non-coincidence of the crystallographic fabric directions with the finite-strain stretching-lineation directions indicates the progressive evolution of the shear system. The textures in the two normal limbs are best interpreted as being associated with the shear movements responsible for the main deformation in the inverted limbs. Continued rotation of shear movements in an anticlockwise sense, that is to a more westerly

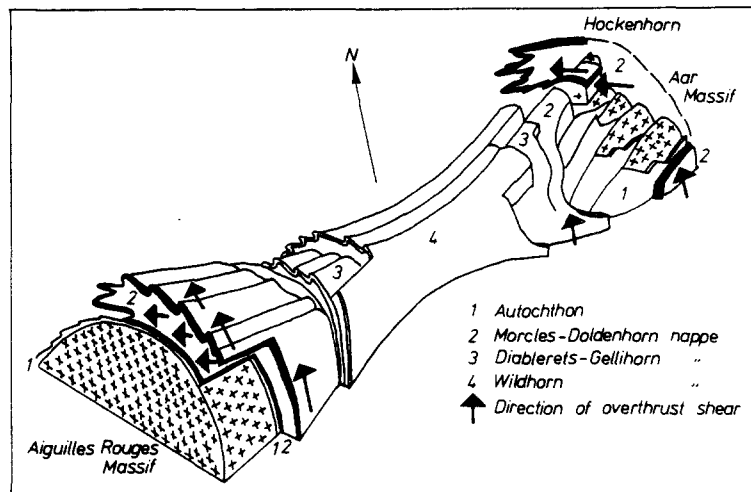


Fig. 12. Block diagram of the Helvetic nappes, showing different overthrust directions in the normal and inverted limbs of the Morcles and of the Doldenhorn nappe. The block diagram is modified after Arbenz, in Heim (1921).

direction, could explain the observed E to W sense of shear deduced from the inverted limb textures.

The final stage of the deformation history is shown by a NE-SW stretching in the root zone. The strain associated with this event is an order of magnitude smaller than that associated with the other two stretching directions (e.g. Casey *et al.* 1983). Dietrich & Song (1984) have shown that there is no direct relationship between this lineation (their L_2) and the crystallographic fabric. One possible explanation of this last event is that it represents the final NE-SW increment in a strain sequence having an overall anticlockwise rotation sense.

Acknowledgements—We thank Martin Casey, John Ramsay, John Ridley and Stefan Schmid for helpful criticism of the text. Dorothee Dietrich feels particularly indebted to Martin Casey for open discussions of his related research, which helped the development of the present paper. G. Mitra and A. W. B. Siddans are thanked for their constructive reviews of the manuscript.

Dorothee Dietrich acknowledges financial support from Schweizerischer Nationalfonds, Project no. 2.325-0.81 (5.521.330.880/5).

REFERENCES

- Bugnon, P. 1981. Géologie des racines helvétiques dans la région de Loèche (Valais). *Bull. Soc. Vaud. Sc. Nat.* 359 75, 201–206.
- Casey, M., Dietrich, D. & Ramsay, J. G. 1983. Methods for determining deformation history for chocolate tablet boudinage with fibrous crystals. *Tectonophysics* 92, 211–239.
- Casey, M. & Huggenberger, P. 1985. Numerical modelling of finite-amplitude similar folds developing under general deformation histories. *J. Struct. Geol.* 7, 103–114.
- Casey, M., Rutter, E. H., Schmid, S. M., Siddans, A. W. B. & Whalley, J. S. 1978. Texture development in experimentally deformed calcite rocks. *Proc. 5th Int. Conf. Textures of Materials*, Springer, Berlin, 231–240.
- Dietrich, D. Calcite fabrics around folds as indicators of the deformation history. *J. Struct. Geol.* (in review).
- Dietrich, D. & Song, H. 1984. Calcite fabrics in a natural shear environment, the Helvetic nappes of western Switzerland. *J. Struct. Geol.* 6, 19–32.
- Dietrich, D., Song, H. & Casey, M. 1981. An attempt at a kinematic interpretation of the root zone of the Helvetic nappes, western Switzerland. *J. Struct. Geol.* 3, 186–187.
- Durney, D. W. 1972. Deformation history of the Western Helvetic nappes, Valais, Switzerland. Unpublished Ph.D thesis, University of London.
- Durney, D. W. & Ramsay, J. G. 1973. Incremental strains measured by syntectonic crystal growths. In: *Gravity and Tectonics* (edited by DeJong, K. & Scholten, R.). Wiley, New York, 67–96.
- Gray, D. R. & Durney, D. W. 1979. Investigations on the mechanical significance of crenulation cleavage. *Tectonophysics* 58, 35–79.
- Heim, A. 1921. *Geologie der Schweiz*, II/1. Tauchnitz, Leipzig.
- Laubscher, H. P. 1983. Detachment, shear, and compression in the central Alps. *Mem. geol. Soc. Am.* 158, 191–211.
- Ramsay, J. G. 1967. *Folding and Fracturing of Rocks*. McGraw-Hill, New York.
- Ramsay, J. G. 1981. Tectonics of the Helvetic nappes. In: *Thrust and Nappe Tectonics* (edited by McClay, K. & Price, N. J.). *Spec. Publ. geol. Soc. Lond.* 9, 293–309.
- Ramsay, J. G., Casey, M. & Kligfield, R. 1983. Role of shear in development of the Helvetic fold-thrust belt of Switzerland. *Geology* 11, 439–442.
- Ramsay, J. G. & Huber, M. 1983. *The Techniques of Modern Structural Geology, Vol. 1: Strain Analysis*. Academic Press, London.
- Schläppi, E. 1980. Geologische und tektonische Entwicklung der Doldenhorn Decke und zugehöriger Elemente. Unpublished Ph.D thesis, University of Bern, Switzerland.
- Schmid, S. M. 1982. Laboratory experiments on rheology and deformation mechanisms in calcite rocks and their application to studies in the field. *Mitt. Geol. Inst. ETH u. Univ. Zürich.* 241, 1–62.
- Schmid, S. M., Casey, M. & Starkey, J. 1981. The microfabric of calcite tectonites from the Helvetic nappes (Swiss Alps). In: *Thrust and Nappe Tectonics* (edited by McClay, K. & Price, N. J.). *Spec. Publ. geol. Soc. Lond.* 9, 151–158.
- Siddans, A. W. B. 1983. Finite strain patterns in some Alpine nappes. *J. Struct. Geol.* 5, 441–448.
- Steck, A. 1984. Structures de déformations tertiaires dans les Alpes centrales. *Eclog. geol. Helv.* 77, 55–100.
- Trümpy, R. 1980. *Geology of Switzerland. Part B: Geological Excursions. Excursion I, Helvetic Alps of Western Switzerland*, by Masson, H., Herb, R. & Steck, A. *Excursion III, Cross section from the Rhine Graben to the Po Plane*, by Laubscher, H. P. & Bernoulli, D. Wepf & Co., Basel, 109–153 and 183–209.